Ab Initio Structure Determination and Dehydration Dynamics of $YK(C_2O_4)_2 \cdot 4H_2O$ Studied by X-ray Powder Diffraction

Thierry Bataille, Jean-Paul Auffrédic, and Daniel Louër*

Laboratoire de Chimie du Solide et Inorganique Moléculaire (U.M.R. C.N.R.S. 6511), Groupe de Cristallochimie, Université de Rennes 1, Avenue du Général Leclerc, 35042 Rennes Cedex, France

Received December 29, 1998. Revised Manuscript Received March 30, 1999

The crystal structure of $YK(C_2O_4)_2 \cdot 4H_2O$ has been solved ab initio from powder diffraction data collected with conventional monochromatic X-rays. The symmetry is tetragonal, space group $I4_1/a$ (no. 88), cell dimensions $a = 11.4612(8)$ Å, $c = 8.9040(8)$ Å, $Z = 4$. The structure is built from chains of oxalate groups bridging 8-fold-coordinated yttrium atoms. The structure has an open framework exhibiting tunnels with square cross-sections, filled with zeolitic water molecules, and ellipsoidal cross-sections in which the potassium atoms are located. The hydrogen atoms have been localized, and their role on the precision of the bond lengths within the oxalate group has been demonstrated. The dehydration process is reversible and occurs with a pronounced anisotropic elastic property of the structure framework. The enthalpy, $\Delta_r H$, and entropy, $\Delta_r S$, of the dehydration reaction have been determined as a function of the number n of zeolitic water molecules. $\Delta_r H$ decreases from 70.2 to 54.2 kJ mol^{-1} during the dehydration process. The crystal structure of a partially hydrated phase, $YK(C_2O_4)_2 \cdot 1.64H_2O$, has also been determined and the relationship between the magnitude of the c parameter of the unit cell and the number n of water molecules has been pointed out. The 8-fold coordination is preserved for yttrium atoms during the dehydration, while it is lowered from eight to less than six for potassium atoms. The complete decomposition scheme into yttrium oxide is reported from thermal analyses studies, including temperature-dependent powder diffraction.

1. Introduction

Mixed oxalate compounds are well-known for their use as precursors in the synthesis of ternary oxides, such as pure barium titanate obtained from the complex thermal decomposition of barium titanyl oxalate hydrate.[1] Recently, oxalates have also been used to produce new open-framework coordination compounds.[2] The presence of cavities in the crystal structure of a number of oxalates has been reported long ago,[3−5] and zeolitic properties arising from weakly bonded water molecules located in these cavities have been discussed.[6] Among mixed oxalates derived from rare earths or yttrium and monovalent cations reported in the literature,[7,8] some phases with different M^I/Ln ratios have been characterized by their crystal structures, e.g., $K_3Ln(C_2O_4)_3 \cdot nH_2O$ (Ln = Nd, Sm, Eu, Gd, Tb),[9] $K_8Ln_2(C_2O_4)_7 \cdot 14H_2O$ (Ln = Tb, Dy, Er, Yb, Y),[10] $NH_4Ln(C_2O_4)_2.nH_2O$ (Y, Sm−Tm),[11] and $MLn(C_2O_4)_2 \cdot nH_2O$ with M = Li, Ln = La···Gd, $n = 2$, or M = Na, Ln = Ce···Nd, $n = 3$.[7] In the course of syntheses of mixed oxalates with yttrium and monovalent cations the phase $YK(C_2O_4)_2 \cdot 4H_2O$ has been prepared here. Although only a powder of this material was obtained, the spectacular progress in powder diffraction that has occurred in the past few years[12] gives an opportunity to investigate moderately complex crystal structures from powder data and to study the thermal behavior of materials in a dynamic mode. The present study deals with the crystal structure of this material, determined ab initio from powder diffraction data collected with conventional monochromatic X-rays, and its thermal behavior, investigated from temperature-dependent powder diffraction. Additionally, the noteworthy behavior of the zeolitic water molecules is discussed from the determination of the crystal structure of a partially dehydrated phase and from the thermodynamic properties of the chemical equilibrium.

(1) Louër, M.; Louër, D.; Gotor, F. J.; Criado, J. M. *J. Solid State Chem.* **1991**, *92*, 565−572.
(2) Ayyappan, S.; Cheetham, A. K.; Natarajan, S.; Rao, C. N. R. *Chem. Mater.* **1998**, *10*, 3746−3755.
(3) Sterling, C. *Nature* **1965**, *205*, 588−589.
(4) Gérard, N.; Watelle-Marion, G.; Thrierr-Sorel, A. *Bull. Soc. Chim. Fr.* **1968**, *11*, 4367−4378.
(5) Hanson, E. *Acta Chem. Scand.* **1970**, *24*, 2969−2982.
(6) Chaix-Pluchery, O.; Mutin, J. C.; Bouillot, J.; Niepce, J. C. *Acta Crystallogr.* **1989**, *C45*, 1699−1705.
(7) Roméro, S.; Mosset, A.; Trombe, J.-C. *Eur. J. Solid State Inorg. Chem.* **1995**, *32*, 1053−1063.
(8) Gencova, O.; Siftar, J. *J. Therm. Anal.* **1997**, *48*, 321−326.
(9) Kahwa, I. A.; Fronczek, F. R.; Selbin, J. *Inorg. Chim. Acta* **1984**, *82*, 161−166.
(10) Kahwa, I. A.; Fronczek, F. R.; Selbin, J. *Inorg. Chim. Acta* **1984**, *82*, 167−172.
(11) McDonald, T. R. R.; Spink, J. M. *Acta Crystallogr.* **1967**, *23*, 944−949.
(12) Langford, J. I.; Louër, D. *Rep. Prog. Phys.* **1996**, *59*, 131−234.

10.1021/cm981155x CCC: $18.00
Published on Web 05/22/1999

2. Experimental Section

Material Preparation. The precipitate of $YK(C_2O_4)_2{\cdot}4H_2O$ was prepared from concentrated solutions to avoid the simultaneous formation of $Y_2(C_2O_4)_3{\cdot}10H_2O$, arising when diluted solutions are used. A pure phase was obtained as follows: 2 mmol of yttrium nitrate pentahydrate (Aldrich no. 23,795-7) and 4 mmol of oxalic acid dihydrate (Prolabo, rectapur no. 20558.365) were dissolved, at room temperature, in 20 mL concentrated nitric acid (Merck A.R. 65%) and a 34% concentrated solution of potassium hydroxide (Prolabo) was added dropwise until the precipitation was complete and the pH of the solution was close to neutrality. At this stage, the temperature of the solution was about 50 °C. The precipitate was filtered off and dried at room temperature. The chemical formula was confirmed from TG analysis, energy dispersive spectrometry (EDS), and the determination of the crystal structure described in the present study.

Collection of High-Resolution Powder X-ray Diffraction Data. High-quality X-ray powder diffraction data were obtained for $YK(C_2O_4)_2{\cdot}4H_2O$ with a Siemens D500 diffractometer using monochromatic Cu Kα_1 radiation (λ = 1.5406 Å) selected with an incident-beam curved-crystal germanium monochromator with asymmetric focusing (short focal distance 124 mm, long focal distance 216 mm). The alignment of the diffractometer was checked by means of the 00*l* reflections of fluorophlogopite mica (NIST SRM 675). The zero error was determined as less than 0.01° (2θ). The instrumental resolution function of the setup exhibits a shallow minimum of 0.065° (2θ) at about 40° (2θ) and has twice this value at 130° (2θ).[13] To reduce preferred orientation effects the powder was mounted in a top-loaded sample holder.[14] The diffraction pattern was scanned over the angular range 10−150° (2θ), with a step length of 0.02° (2θ) and a counting time of 20 s step^{-1} until 56° (2θ), 40 s step^{-1} from 56.02° (2θ) to 101° (2θ), and 80 s step^{-1} to the end of the scan. Then, the full pattern was scaled to 20 s step^{-1}. After data collection, the stability of the X-ray source was checked by recording again the diffraction lines at low angles.

Diffraction data for a partially dehydrated phase were also collected at room temperature from a sample kept under a flowing nitrogen atmosphere by using a tight sample holder. The pattern was scanned over the angular range 10−120° (2θ), with a step size of 0.02° (2θ) and a counting time of 30 s step^{-1} until 80° (2θ) and 60 s step^{-1} to the end of the scan. Data were then scaled to 30 s step^{-1}. A correction of intensities collected at angles below 20° (2θ) was applied from the changes in integrated intensities obtained for data collected with a narrower receiving slit.

Precise in situ powder diffraction data were collected as a function of temperature under a partial water-vapor pressure of 9.5 Torr with an old automated Siemens diffractometer equipped with a graphite diffracted beam monochromator operating with Co Kα radiation (λ Kα_1 = 1.7890 Å, λ Kα_2 = 1.7929 Å) and a high-temperature attachment. The water-vapor pressure was generated by bubbling nitrogen in a sulfuric acid solution with a concentration of 7.06 mol L^{-1} and kept at 18 °C.

The extraction of peak positions for indexing was performed with the Socabim fitting program PROFILE, available in the PC software package DIFFRAC-AT supplied by Siemens. Pattern indexing was carried out by means of the program DICVOL91.[15] The programs EXTRA[16] and SIRPOW.92[17] were used for structure solution and FULLPROF[18] for structure refinement by the Rietveld method. The programs POWDER CELL 1.0[19] and WebLab ViewerLite from Molecular Simulations Inc. were used for structure drawings.

Thermal Analyses. Temperature-dependent X-ray diffraction (TDXD) was performed with a powder diffractometer combining the curved position sensitive detector (PSD) from INEL (CPS 120) and a high-temperature attachment from Rigaku. The detector was used in a semifocusing arrangement by reflection (Cu Kα_1 radiation) as described elsewhere.[20] With this geometry the flat sample is stationary. An angle of 6° between the incident beam and the surface of the sample was selected. The thermal decomposition of $YK(C_2O_4)_2{\cdot}4H_2O$ was carried out under a partial water-vapor pressure of 5.5 Torr with a heating rate of 15 °C h^{-1} to 600 °C. To ensure satisfactory counting statistics, a counting time of 1500 s per pattern was selected. Thermal dehydration was carried out under a partial water-vapor pressure of 5.5 Torr under flowing nitrogen, as described above. A regime of 6 °C h^{-1}, combined with a counting time of 2400 s per pattern, was selected for the thermal treatment.

TG analyses were carried out with a Rigaku Thermoflex instrument under a partial water-vapor pressure of 5.5 Torr with a heating rate of 10 °C h^{-1} until 900 °C and also with a MacBain thermobalance under selected water-vapor pressures. The powdered samples were spread evenly in a large platinum crucible to avoid mass effects.

3. Ab Initio Structure Determination of $YK(C_2O_4)_2{\cdot}4H_2O$

Pattern Indexing. The first 20 lines of the X-ray powder diffraction pattern, with an absolute error of 0.03° (2θ) on peak positions, were indexed on the basis of a tetragonal solution with the figures of merit M_{20} = 35 and F_{20} = 43 (0.0080, 58) (see ref 12). The correctness of this solution was confirmed from an analysis of the powder data available. After this evaluation and refinement, the unit cell dimensions were a = 11.4612(8) Å, c = 8.9040(8) Å, and V = 1169.6(2) Å^3 with M_{20} = 62 and F_{30} = 80 (0.0093, 40) according to the conditions for nonextinction. The powder data have been submitted to the ICDD[21] for possible inclusion in the Powder Diffraction File. The reflection conditions uniquely identified space group $I4_1/a$ (no. 88).

Structure Determination. Integrated intensities were extracted with the program EXTRA. In the angular range 10−110° (2θ), 371 structure-factor amplitudes were obtained, including 35.0% of statistically independent reflections, according to the degree of diffraction line overlap.[22] They were used as input in the direct-methods program SIRPOW.92. All but the hydrogen atoms were found from the first six maxima in the E-map with the highest figure of merit. Among the six atoms in the asymmetric unit both the yttrium and the potassium atoms lie on special positions. The refinement of the atomic coordinates of C and O led to a residual value R = 9.5%. At this stage, the molecular geometry displayed by the program SIRPOW.92 was in agreement with the presence of oxalate groups bonded

(13) Louër, D.; Langford, J. I. *J. Appl. Crystallogr.* **1988**, *21*, 430−437.
(14) Swanson, H. E.; Morris M. C.; Evans, E. H.; Ulmer, L. *Natl. Bur. Stand.* (*U.S.*) **1964**, Monogr. 25, Section 3, pp 1−3.
(15) Boultif, A.; Louër, D. *J. Appl. Crystallogr.* **1991**, *24*, 987−993.
(16) Altomare, A.; Burla, M. C.; Cascarano, G.; Giacovazzo, C.; Guagliardi, A.; Moliterni, A. G. G.; Polidori, G. *J. Appl. Crystallogr.* **1995**, *28*, 842−846.
(17) Altomare, A.; Cascarano, G.; Giacovazzo, C.; Guagliardi, A.; Burla, M. C.; Polidori, G.; Camalli, M. *J. Appl. Crystallogr.* **1994**, *27*, 435−436.
(18) Rodriguez-Carvajal, J. In *Collected Abstracts of Powder Diffraction Meeting*, Toulouse, France, p 127−128, 1990.
(19) Kraus, W.; Nolze, J. *J. Appl. Crystallogr.* **1996**, *29*, 301−303.
(20) Plévert, J.; Auffrédic, J. P.; Louër, M.; Louër, D. *J. Mater. Sci.* **1989**, *24*, 1913−1918.
(21) PDF Database; International Centre for Diffraction Data: Newton Square, PA.
(22) Altomare, A.; Cascarano, G.; Giacovazzo, C.; Guagliardi, A.; Moliterni, A. G. G.; Burla, M. C.; Polidori, G. *J. Appl. Crystallogr.* **1995**, *28*, 738−744.

Table 1. Crystallographic Data and Details of the Rietveld Refinements[a]

	$YK(C_2O_4)_2 \cdot 4H_2O$	$YK(C_2O_4)_2 \cdot 1.64H_2O$
space group	$I4_1/a$	$I4_1/a$
Z	4	4
wavelength (Å)	1.5406	1.5406
2θ range (deg)	10−150	10−120
step scan increment (deg 2θ)	0.02	0.02
no. of atoms	8	6
no. of reflections	614	417
no. of structural parameters	19	15
no. of profile parameters	16	27
R_F	0.037	0.071
R_B	0.058	0.078
R_P	0.094	0.115
R_{WP}	0.125	0.150
R_{exp}	0.051	0.057

[a] For the definition of the R factors, see ref 12.

to yttrium atoms and water molecules coordinated to potassium atoms. A least-squares Rietveld refinement using the program FULLPROF was carried out in the complete angular range 10−150° (2θ) containing 614 reflections. A pseudo-Voigt function was selected to describe individual line profiles, with a possible variation of the mixing factor η. The refinement involved the following parameters: 18 atomic parameters (including 6 isotropic atomic displacement parameters), 1 scale factor, 1 zero-point, 2 cell parameters, 3 half-widths and 2 line asymmetry parameters, 2 variables for the angular variation of η, 1 preferred orientation parameter, and 5 polynomial background coefficients. Although the refinement converged to satisfactory residual factors, $R_F = 0.040$ and $R_{wp} = 0.129$, some distortions were observed within the oxalate groups, i.e., the C−C and C−O mean distances were 1.61(1) and 1.226(9) Å, respectively. At this stage, a last difference Fourier map revealed a low residual electron-density (0.15 e $Å^{-3}$) in the vicinity of the water oxygen atom. The distance was found compatible with a H atom. Consequently, the position of the second hydrogen atom was calculated according to the geometry of the water molecule and to the hydrogen bonds criteria used by Baur and Khan.[23] The final Rietveld refinement was carried out including the hydrogen atoms as fixed contributions, with an isotropic atomic displacement parameter fixed to 4.0 $Å^2$. Then, the final reliability factors were $R_F = 0.037$ and $R_{wp} = 0.125$ and, as discussed later on, the distances within the oxalate group [C−C distance: 1.533(9) Å, C−O distances: 1.266(8) Å and 1.269(9) Å] were in good agreement with the values reported in the literature. Crystallographic data and details of the Rietveld refinement are given in Table 1. Figure 1 shows the best agreement obtained between calculated and observed patterns. Final atomic position parameters are given in Table 2 and selected distances and angles are listed in Table 3.

Description of the Structure. The structure of $YK(C_2O_4)_2 \cdot 4H_2O$ is built from zigzag chains of oxalate groups bridging the yttrium atoms and running along [100] and [010]. As shown in Figure 2a, the resulting

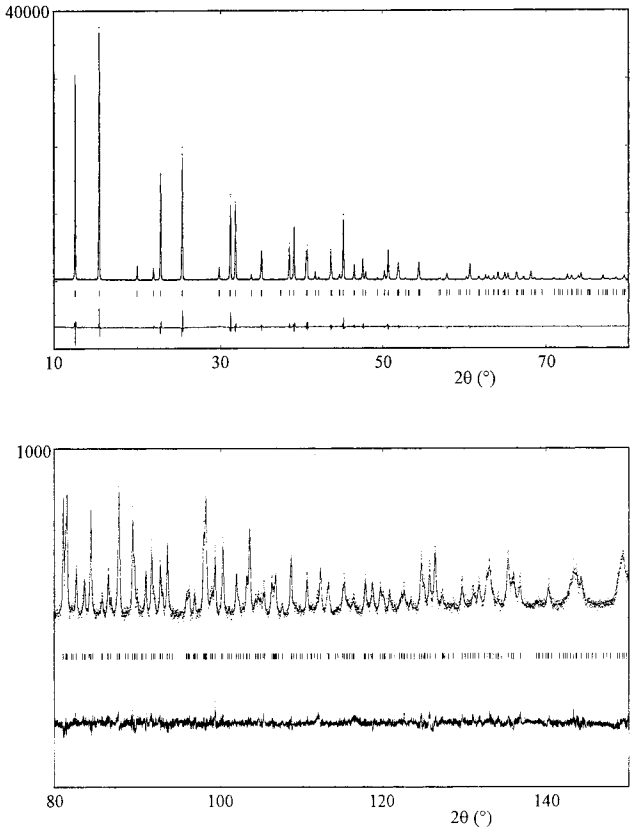

Figure 1. Final Rietveld refinement plot for $YK(C_2O_4)_2 \cdot 4H_2O$. The experimental data are represented by dots, while the calculated pattern is shown by the solid line. The lower trace corresponds to the difference curve between observed and calculated patterns. The Bragg reflections are shown by the vertical bars. Note that the intensity scale is magnified for the high-angle region.

open framework exhibits tunnels parallel to the c axis with a square cross section, in which are located the water molecules. Figure 3 is a projection of the structure along [010]. It shows the presence of ellipsoidal tunnels, built from six-membered rings $[Y(C_2O_4)]_6$ formed by the oxalate groups [two of them are perpendicular to (010)] and the yttrium atoms, in which are located the potassium atoms. Similar ellipsoidal tunnels are also running along [100] and along ⟨111⟩. It must be noted that this topology has been found in the structure of some oxalates[5,24] and that six-membered rings, in which cations are located, are also found in silicates, e.g., in the structure of petarasite.[25]

The yttrium atom is 8-fold-coordinated by the oxalate oxygen atoms only (Figure 4), in a slightly distorted triangulated dodecahedron. This bisdisphenoid is made up from a squashed tetrahedron formed by the O1 atoms and an elongated one formed by the O2 atoms. According to Hyde and Andersson,[26] for this kind of coordination the Y−O1 distance [2.338(7) Å] is normally shorter than the Y−O2 distance [2.381(5) Å]. The range of distances Y−O are comparable to the values reported for similar 8-fold-coordinated yttrium atoms in related

(23) Baur, W. H.; Khan, A. A. *Acta Crystallogr.* **1970**, *B26*, 1584−1596.

(24) Roméro, S.; Mosset, A.; Trombe, J.-C. *J. Solid State Chem.* **1996**, *127*, 256−266.

(25) Rocha, J.; Ferreira, P.; Lin, Z.; Agger, J. R.; Anderson, M. W. *Chem. Commun.* **1998**, 1269−1270.

(26) Hyde, B. G.; Andersson, S. *Inorganic Crystal Structures*; Wiley-Intersciences: New York, 1989.

Table 2. Fractional Atomic Coordinates and Isotropic Atomic Displacement Parameters (Å²) for $YK(C_2O_4)_2 \cdot 4H_2O$[a]

	Wyckoff site	*x*		*y*		*z*		B_{iso}
Y	4b	0	[0]	1/4	[1/4]	5/8	[5/8]	1.14(3)
K	4a	0	[0]	1/4	[1/4]	1/8	[1/8]	2.17(8)
O1	16f	0.1985(4)	[0.2013(8)]	0.2579(8)	[0.244(2)]	0.5660(5)	[0.5654(9)]	1.7(1)
O2	16f	0.1177(3)	[0.1209(5)]	0.2357(7)	[0.251(2)]	0.8444(5)	[0.862(1)]	1.0(1)
C	16f	0.2735(6)	[0.2753(6)]	0.248(2)	[0.261(2)]	0.6695(7)	[0.6717(8)]	1.3(2)
Ow	16f	0.2958(5)	[0.314(3)]	0.3913(5)	[0.186(2)]	0.3311(7)	[0.267(2)]	3.9(2)
H1	16f	0.2509		0.3410		0.3852		4.0
H2	16f	0.2475		0.4136		0.2529		4.0

[a] The values obtained for $YK(C_2O_4)_2 \cdot 1.64H_2O$ are reported in square brackets. Note: An overall isotropic atomic displacement parameter was refined for $YK(C_2O_4)_2 \cdot 1.64H_2O$, $B_{ov} = 1.14(7)$ Å². The site occupancy factor of Ow for the phase $YK(C_2O_4)_2 \cdot 1.64H_2O$ was refined to 0.41(1).

Table 3. Selected Bond Distances (Å) and Angles (deg) for $YK(C_2O_4)_2.4H_2O$[a]

Y−O1, $O1^{i}$, $O1^{ii}$, $O1^{iii}$	2.338(7)	O2−$O2^{i}$	2.719(6)
Y−O2, $O2^{i}$, $O2^{ii}$, $O2^{iii}$	2.381(5)	$O2^{iv}$−Ow^{ix}	3.286(9)
K−$O2^{ii}$, $O2^{iii}$, $O2^{iv}$, $O2^{v}$	2.846(5)	$O2^{iv}$−Ow^{vi}	3.386(8)
K−Ow^{vi}, Ow^{vii}, Ow^{viii}, Ow^{ix}	2.873(5)	$O2^{iv}$−Ow^{viii}	4.243(8)
C−O1	1.266(8)	Ow^{vi}−Ow^{viii}, Ow^{ix}	4.101(8)
C−$O2^{x}$	1.269(9)	Ow−Ow^{ix}, Ow^{xi}	2.937(8)
C−C^{x}	1.533(9)	Ow−H1	0.911(6)
O1−$O1^{ii}$, $O1^{iii}$	3.39(1)	Ow−H2	0.927(6)
O1−O2	2.661(6)	H1···O1	1.966(6)
O1−$O2^{iii}$	2.845(8)	H2···Ow^{ix}	2.011(6)
O1−$O2^{ii}$	3.173(8)		
O1−Y−$O1^{ii}$	92.9(4)	O1−C−$O2^{x}$	125.6(7)
O1−Y−O2	68.6(2)	O1−C−C^{x}	116.1(8)
O1−Y−$O2^{iii}$	74.1(3)	$O2^{x}$−C−C^{x}	115.6(8)
O1−Y−$O2^{ii}$	84.5(3)	K^{xi}−Ow−H1	91.9(4)
O2−Y−$O2^{i}$	69.6(2)	K^{xi}−Ow−H2	138.2(4)
$O2^{ii}$−K−$O2^{iii}$	57.1(3)	H1−Ow−H2	103.5(5)
$O2^{ii}$−K−Ow^{vii}	70.1(2)	$H2^{xi}$···Ow−K^{xi}	92.8(2)
$O2^{ii}$−K−Ow^{ix}	72.6(2)	$H2^{xi}$···Ow−H1	96.4(4)
$O2^{ii}$−K−Ow^{vi}	95.8(3)	$H2^{xi}$···Ow−H2	122.9(4)
Ow^{vi}−K−Ow^{viii}	91.1(3)	Ow−H1···O1	155.9(8)
Ow−H2···Ow^{ix}	177.3(8)		

[a] Geometry of the water molecule is described according to the classification reported by Ferraris and Franchini-Angela (ref 29): (i) $-x, 1/2 - y, z$; (ii) $-1/4 + y, 1/4 - x, 5/4 - z$; (iii) $1/4 - y, 1/4 + x, 5/4 - z$; (iv) $x, y, -1 + z$; (v) $-x, 1/2 - y, -1 + z$; (vi) $1/2 - x, 1/2 - y, 1/2 - z$; (vii) $-1/2 + x, y, 1/2 - z$; (viii) $1/4 - y, -1/4 + x, -1/4 + z$; (ix) $-1/4 + y, 3/4 - x, -1/4 + z$; (x) $1/2 - x, 1/2 - y, 3/2 - z$; (xi) $3/4 - y, 1/4 + x, 1/4 + z$.

oxalates, e.g., 2.311−2.393 Å for $Y_2(C_2O_4)_3 \cdot 6H_2O$,[27] 2.265−2.455 Å for $Y_2(C_2O_4)_3 \cdot 3H_2O$,[27] 2.299−2.386 Å for $K_8Y_2(C_2O_4)_7 \cdot 14H_2O$.[10] This is also confirmed by the calculation of bond distances performed with the program VALENCE,[28] i.e., 2.382 Å for 8-fold-coordinated Y atom. The O1−O2 edges have three sets each of four equidistant bonds. The lengths of the edges of the dodecahedron vary from 2.661(6) to 3.39(1) Å.

The potassium atom is 8-fold-coordinated by four oxalate oxygen atoms and four water oxygen atoms. The resulting polyhedron is also a distorted triangulated dodecahedron. The squashed tetrahedron of this bisdisphenoid is formed by the water molecules and the elongated tetrahedron by the O2 atoms. However, the K−Ow distance [2.873(5) Å] is not shorter than the K−O2 distance [2.846(5) Å], as it could be expected from the ideal polyhedron.[26] Similar bond lengths are reported for 8-fold-coordinated potassium atom, e.g., 2.79−3.11 Å for $K_8Y_2(C_2O_4)_7 \cdot 14H_2O$,[10] in which the coordination sphere is also made from four oxalate oxygen atoms and four water oxygen atoms. The distances agree well with the calculated value obtained from the program VALENCE[28] for 8-fold-coordinated potassium atom, i.e., 2.901 Å. As it is observed in the yttrium coordination environment, the O2−Ow distances split in three sets, in the range 3.286(9)−4.243(8) Å. The edge lengths of the dodecahedron vary from 2.719(6) Å to 4.243(8) Å. The potassium and yttrium coordination polyhedra share their O2−O2 edges as shown in Figure 4 and form a chain parallel to the *c* axis. The unit cell

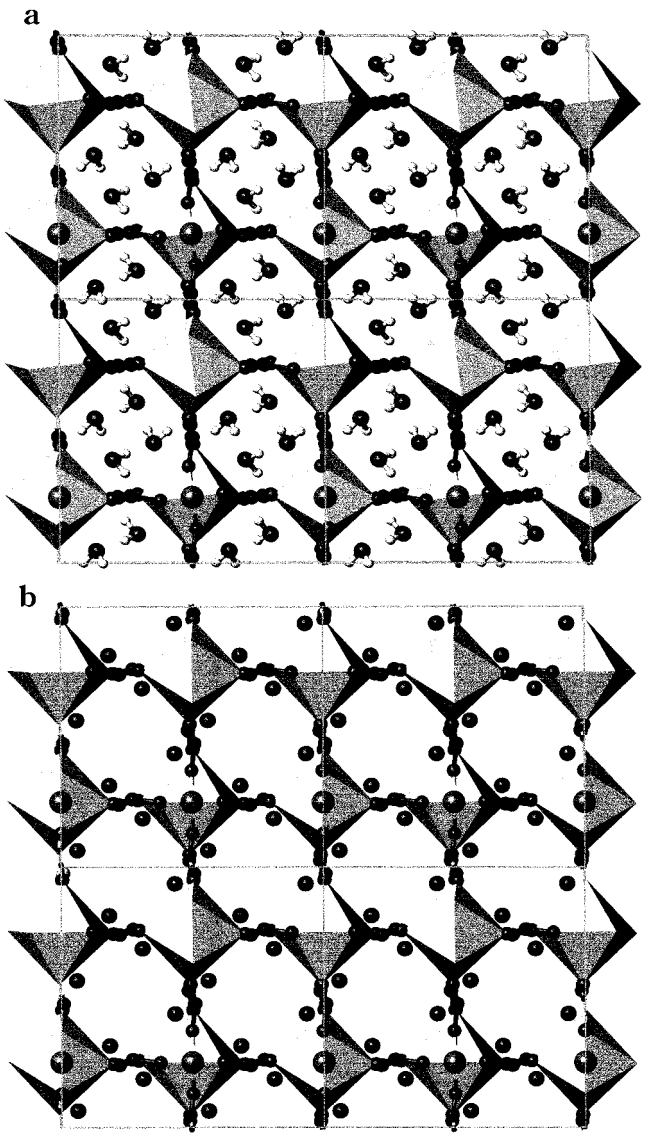

Figure 2. Projection of the structures along the *c* axis of (a) $YK(C_2O_4)_2 \cdot 4H_2O$ and (b) $YK(C_2O_4)_2 \cdot 1.64H_2O$, showing the polyhedra YO_8 linked by oxalate groups and the water molecules in the tunnels, large dark circle. K: (a) horizontal and (b) vertical.

(27) Picard, V. Ph.D. Thesis, Université de Bourgogne, France, 1993.
(28) Brown, I. D. *J. Appl. Crystallogr.* **1996**, *29*, 479−480.

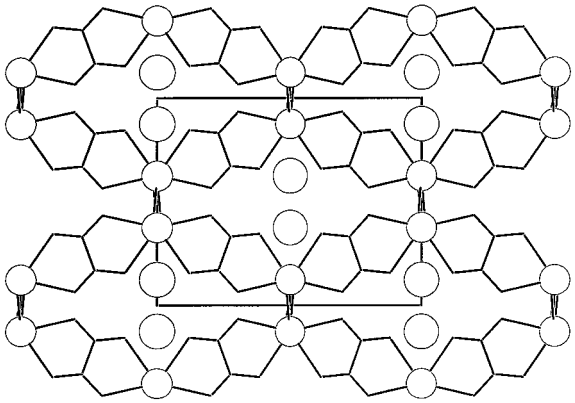

Figure 3. The six-membered rings $[Y(C_2O_4)]_6$ in the structure of $YK(C_2O_4)_2 \cdot 4H_2O$, viewed along the *b* axis. The potassium atoms are shown inside the ellipsoidal tunnels; water molecules are omitted for clarity.

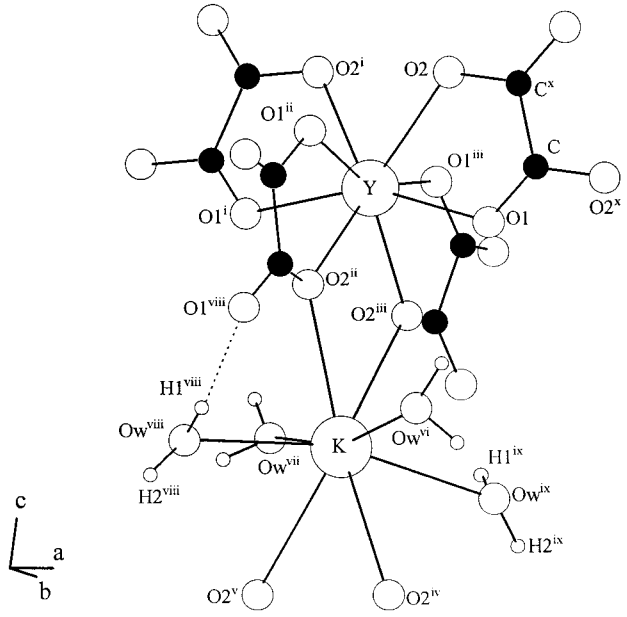

Figure 4. Environment of the yttrium and the potassium atoms in $YK(C_2O_4)_2 \cdot 4H_2O$.

contains four chains located at (0, $^1/_4$, *z*), (0, $^3/_4$, *z*), ($^1/_2$, $^1/_4$, *z*) and ($^1/_2$, $^3/_4$, *z*) linked together by oxalate groups only.

The oxalate groups are bidentate and bridge the yttrium atoms. Bond lengths within the oxalate anion agree well with those found in various carboxylate compounds. The C−C distance is 1.533(9) Å, the average C−O distance is 1.268(9) Å and the mean O−C−C angle is 115.9(8)°. For comparison, the bond lengths and angles within the bridging C_2O_4 group reported for $K_8Y_2(C_2O_4)_7 \cdot 14H_2O$ are 1.543(7) Å for the C−C distance, 1.241(5)−1.247(5) Å for the C−O distances and 116.4(5)−117.3(4) ° for the O−C−C angles.[10] The centers of the oxalate anions coincide with centers of symmetry, at (0, 0, $^1/_2$) and its symmetrically equivalent points of the space group. The oxalate group is almost planar, the deviation calculated from the mean-plane is 0.05 Å. Moreover, the dihedral angle between the mean-plane and (100) or (010) is 4.8° only, and the oxalate groups have their normals close to [100] and [010]. Hence, due to the tetragonal symmetry, oxalate anions form square tunnels in the [001] direction.

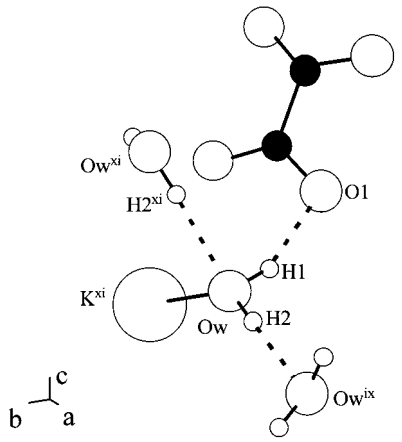

Figure 5. Environment of a water molecule in $YK(C_2O_4)_2 \cdot 4H_2O$. The hydrogen bonds are shown by the dotted lines.

The four water molecules of the formula unit are symmetrically distributed in the square tunnels and all coordinate only the potassium atoms. Thus, no bonds are involved between water molecules and yttrium atoms, since the shortest distance is 4.581(6) Å. The Ow−Ow distances are 4.101(8) Å within a potassium coordination sphere and 2.937(8) Å between two water molecules of adjacent polyhedra, which also are the nearest water molecules in the square tunnels. Figure 5 shows the environment of a water molecule. Hydrogen bonds are clearly defined since the hydrogen atoms were located. The H1−Ow−H2 angle, 103.5(5)°, is close to the ideal value of the tetrahedral angle. Ow is hydrogen-bonded both to O1 via H1 and to Ow^{ix} via H2. The H1···O1 and H2···Ow^{ix} distances are 1.966(6) and 2.011(6) Å, respectively. The K^{xi}−Ow−H1 and K^{xi}−Ow−H2 angles [91.9(4)° and 138.2(4)°, respectively] are far from a tetrahedral angle. The Ow−H−$O_{(acceptor)}$ angles are slightly bent, i.e., 155.9(8)° for Ow−H1−O1 and 177.3(8)° for Ow−H2−Ow^{ix}. Since the environment of the water oxygen atom is well-defined, it is of interest to describe the geometry of the water molecule according to the classification reported by Ferraris and Franchini-Angela.[29] This classification is related to the number and the nature of coordinated cations and to the positions of the cations with respect to the lone pair orbitals of the water oxygen atoms. As shown in Figure 5, Ow coordinates K^{xi} and $H2^{xi}$. The expected classification of the water molecule is then type G from class 2. According to these authors, π is the plane defined by Ow, H1, and H2 and π_1 is the plane defined by Ow, K^{xi}, and $H2^{xi}$. The angles K^{xi}−Ow−π and $H2^{xi}$−Ow−π are 39.2° and 53.3°, respectively. The angle between π and π_1 is 93.9°, thus the two planes are almost perpendicular. These results are in agreement with a water molecule from the class 2 and the type G of the classification. Nevertheless, the K^{xi}−Ow−H2 angle is 92.8(2)°, while it should be close to the ideal value in a tetrahedron. Moreover, the intersection between π and π_1, called Δ, is far from the bisector of the H1−Ow−H2 angle, i.e., the angles Δ−Ow−H1 and Δ−Ow−H2 are 84.4° and 19.3°, respectively. Similar discrepancies have been reported for $NaAl(SO_4)_2 \cdot 12H_2O$.[29]

(29) Ferraris, G.; Franchini-Angela, M. *Acta Crystallogr.* **1972**, *B28*, 3572−3583.

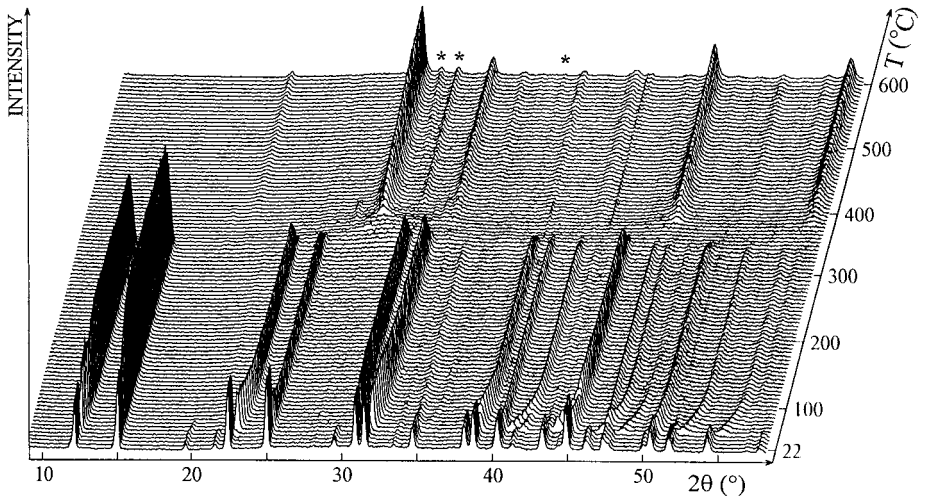

Figure 6. TDXD plot for $YK(C_2O_4)_2{\cdot}4H_2O$ under a partial water-vapor pressure of 5.5 Torr (heating rate, 15 °C h^{-1}; counting time,1500 s per pattern). The asterisks (*) indicate diffraction lines of K_2CO_3.

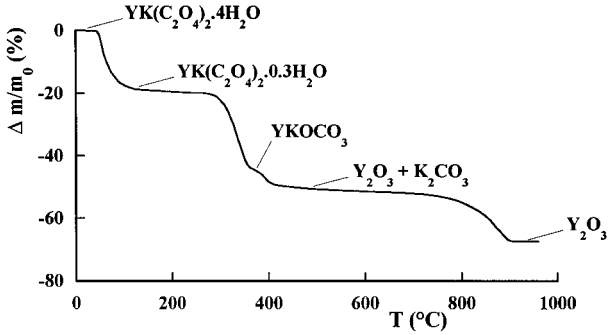

Figure 7. TG curve for the decomposition of $YK(C_2O_4)_2{\cdot}4H_2O$ under a partial water-vapor pressure of 5.5 Torr (heating rate, 10 °C h^{-1}).

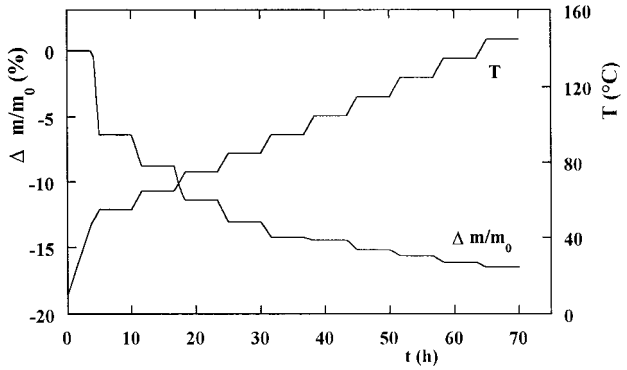

Figure 8. TG curve for the dehydration of $YK(C_2O_4)_2{\cdot}4H_2O$ under a water-vapor pressure of 5.5 Torr, showing that the water content is constant at a given temperature.

4. Thermal Behavior and Dehydration Dynamics

Thermal Decomposition. Figure 6 shows the three-dimensional representation of the successive X-ray powder diffraction patterns obtained during the thermal decomposition of $YK(C_2O_4)_2{\cdot}4H_2O$ heated at 10 °C h^{-1} under a partial water-vapor pressure of 5.5 Torr. The corresponding TG curve is displayed in Figure 7. These figures show that the dehydration starts at about 45 °C and it involves a dramatic change of some diffraction lines. The weight loss reaches 17.8% at 90 °C, corresponding to the departure of ~3.7 water molecules per formula unit. It is accompanied with a continuous shift of the diffraction lines. In the temperature range 90−250 °C, the rate of the dehydration is very low and the remaining water is lost in a much more gradual process. The removal of the last amount of water molecules coincides with the onset of the decomposition which takes place above 300 °C.

The decomposition of the anhydrous material leads to an amorphous phase in the narrow domain of temperature 350−370 °C (Figure 6). The end of this decomposition is marked by an inflection on the TG curve, where the weight loss of about 44% is in accordance with the formation of a solid for which the global composition is $YKOCO_3$ (theoretical weight loss 42.4%). Between 370 and 400 °C, the lines of Y_2O_3 and some other lines emerge from the background. As seen in Figure 6, these lines with low intensity disappear above 410 °C. Subsequently the intensity of the diffraction lines of Y_2O_3 increases and some new lines with low intensity appear above 410 °C. As demonstrated from additional TDXD experiments carried out with pure K_2CO_3 these additional lines belong to the high-temperature hexagonal modification of this compound (PDF file no. 27-1348).[21] The formation of an equimolar mixture of the two phases Y_2O_3 and K_2CO_3 is in good agreement with the weight loss observed at 500 °C on the TG curve (experimental 51%; theoretical 51.6%). This mixture of phases loses weight slowly up to 750 °C and then decomposes more quickly to give a final stable plateau at 69% above 900 °C. This total weight loss corresponds to the formation of pure Y_2O_3 as pointed out by the diffraction pattern of the residue (theoretical weight loss 70.0%). The decomposition of K_2CO_3 in the mixture from 750 °C is rather surprising, since it is known that pure potassium carbonate decomposes only above its melting point (891 °C), even when it is mixed with a stoichiometric amount of Y_2O_3, as demonstrated by complementary TG measurement.

Dehydration Dynamics. To describe thoroughly the dynamic dehydration process, experiments were carried out under selected water-vapor pressures. Figure 8 displays the TG curve obtained under a water-vapor pressure of 5.5 Torr, with temperature stages scanned every 10 °C over the range 45−145 °C. It shows that a plateau is immediately obtained as soon as a selected temperature is achieved. Furthermore, it has been

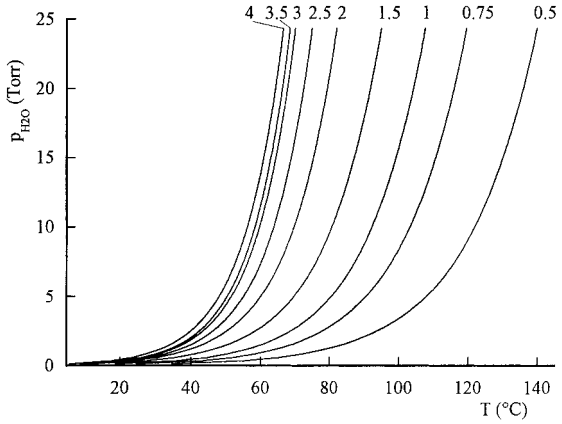

Figure 9. Equilibrium dehydration curves for different water contents ($4 > n > 0.5$) in $YK(C_2O_4)_2 \cdot nH_2O$.

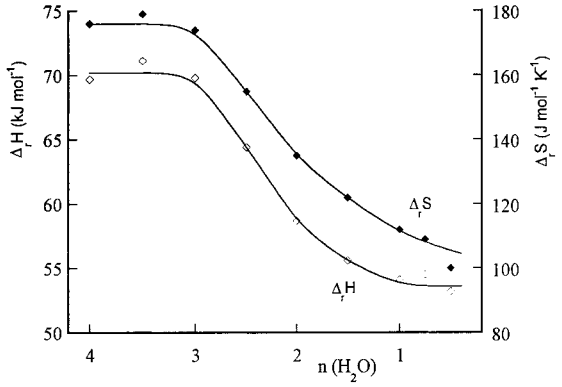

Figure 10. Dependence of the enthalpy and the entropy of dehydration (calculated for 1 mol of water) with the number of water molecules in the material.

shown that the rehydration reaction takes place very quickly upon cooling. Consequently, the water content in the oxalate material depends on both the water-vapor pressure and the temperature, according to a divariant system. The water molecules located inside the structure framework can then be considered as zeolitic water.

From the TG measurements carried out under different water-vapor pressures it is easy to determine the equilibrium $P(H_2O)$ at different temperatures T, for a given value n. The equilibrium dehydration curves $P(H_2O)-T$ for different values of n are shown in Figure 9. $P(H_2O)$ fits the general relationship

$$\ln P(H_2O) = (A/T) + B$$

From the slope A and the intercept B the values of the enthalpy $\Delta_r H$ and the entropy $\Delta_r S$ of the dehydration reaction were calculated for the loss of one water molecule. Figure 10 shows the dependence of $\Delta_r H$ and $\Delta_r S$ with the number n of water molecules in the material. It can be seen that $\Delta_r H$ and $\Delta_r S$ decrease in the course of dehydration. The enthalpy of dehydration decreases from about 70.2 to 54.2 kJ mol^{-1}, which is close to the mean value 55.2 kJ mol^{-1} observed for a large number of hydrated salts.[30] This value compares well with the enthalpy of sublimation of solid water (52.09 kJ mol^{-1}). This is consistent with a lowering of the bond strength involving the water molecules and a relatively unchanged structure framework during dehydration.

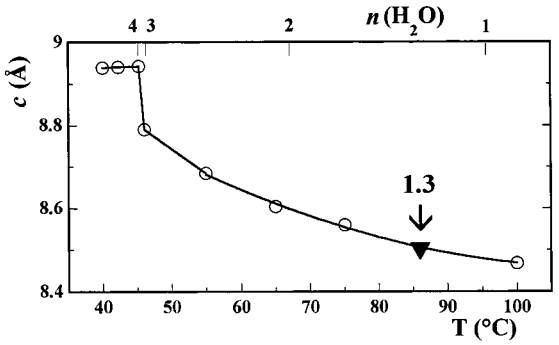

Figure 11. Behavior of the c parameter as a function of temperature and number n of water molecules. The water content ($1.3H_2O$) ascribed to the c parameter value obtained from the Rietveld refinement of the structure of $YK(C_2O_4)_2 \cdot 1.64H_2O$ is also reported.

Additional in situ diffraction experiments were carried out under a partial water vapor pressure of 9.5 Torr. Patterns were indexed with tetragonal unit cells (space group $I4_1/a$) and similar unit cell parameters as obtained for $YK(C_2O_4)_2 \cdot 4H_2O$. Unit cell parameters were obtained from the pattern-matching option supplied by the program FULLPROF. Figure 11 represents the changes of the c axis [from 8.939(6) to 8.4678(9) Å] in the temperature range 40−100 °C. The dehydration process is accompanied with a continuous decrease of the c parameter from $n(H_2O) \sim 3$, while the a parameter remains almost constant over the temperature range [from 11.4840(6) to 11.441(1) Å]. Figure 12 displays the successive powder diffraction patterns obtained with the PSD upon heating to 200 °C and then upon cooling to room temperature. The contraction of the c axis is clearly displayed by the strong shifts of the hkl ($l \neq 0$) lines to higher angles, whereas the $hk0$ lines are very little affected by the transformations. Moreover, it shows that the dehydration process is perfectly reversible, since the patterns obtained upon cooling at room temperature are attributed to $YK(C_2O_4)_2 \cdot 4H_2O$. It is worth noting the remarkable anisotropic elasticity of the structure framework.

Structure Refinement of a Partially Dehydrated Phase. Since in situ diffraction data obtained upon heating were not good enough for precise structure refinement, a sample of a partially dehydrated material was obtained at room temperature under flowing nitrogen. The pattern was indexed with a tetragonal unit cell, with parameters comparable with those obtained for the tetrahydrated phase, i.e., $a = 11.4918(8)$ Å, $c = 8.4972(8)$ Å, $V = 1122.1(2)$ Å^3 [$M_{20} = 66$, $F_{30} = 78(0.010,37)$]. A preliminary examination of the pattern revealed anisotropic diffraction line broadening as shown in Figure 13. Reflections $hk0$ lines are on average broader than hkl ($l \neq 0$) lines. This observation was modeled in the Rietveld refinement by using two functions to describe the angular dependence of the peak width and shape. The refinement was carried out with the program FULLPROF on the basis of the non-hydrogen atomic positions obtained for the tetrahydrated phase. Due to the fact that the water molecule content of the sample was not precisely determined,

(30) Grindstaff, W. K.; Fogel, N. *J. Chem. Soc., Dalton Trans.* **1972**, 1476−1481.

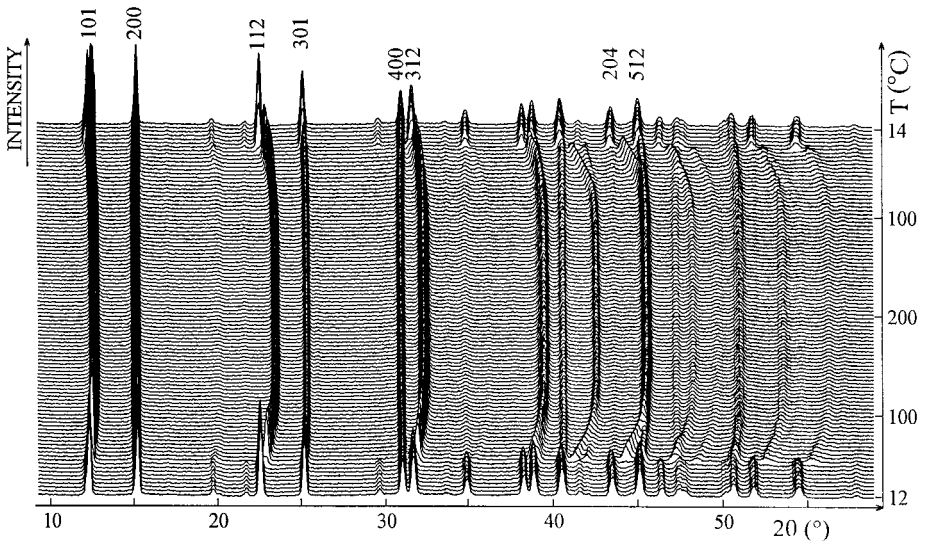

Figure 12. TDXD plot for $YK(C_2O_4)_2 \cdot 4H_2O$ showing the reversible thermal dehydration/hydration under a partial water-vapor pressure of 5.5 Torr (heating and cooling rates: 6 °C h^{-1}; counting time: 2400 s per pattern). Some representative diffraction lines are indexed to point out the significant change of the *c* parameter with temperature.

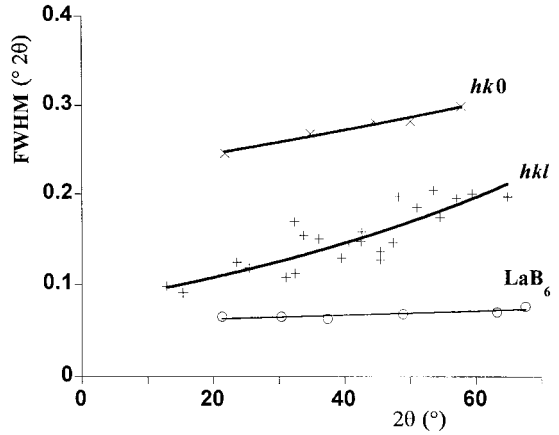

Figure 13. Anisotropic diffraction line broadening of the *hk*0 Bragg reflections in the pattern of $YK(C_2O_4)_2 \cdot 1.64H_2O$. The angular dependence of the fwhm of the standard reference material LaB_6 (NIST-SRM 660) is shown for comparison.

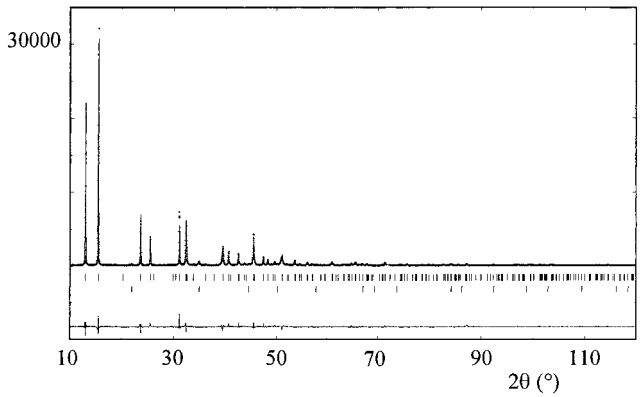

Figure 14. Final Rietveld plot for $YK(C_2O_4)_2 \cdot 1.64H_2O$, showing the observed, calculated and difference profiles. The Bragg reflections are indicated by the vertical bars, the lower bars correspond to the *hk*0 reflections modeled separately in the Rietveld refinement.

several refinements were carried out with different fixed water molecule occupancies. This trial-and-error approach was used to avoid false-minimum problems when refining the unstable site-occupancy factor of the water molecule. The best fit was distinctly obtained for a site occupancy of 0.4. At this stage, the water-occupancy factor was subsequently refined and the final refinement converged to 0.41(1), i.e., 1.64 ± 0.12 water molecules per chemical formula. The details of the Rietveld refinement are given in Table 1 and the final Rietveld plot in Figure 14. Atomic positions, site-occupancy factors and the overall isotropic displacement parameter are given in Table 2. Bond distances and angles are listed in Table 4. It should be noted that due to the sensitivity of the refinement of the partially occupied water molecule site, combined with low-resolution diffraction data ($\sin\theta/\lambda < 0.56$ Å^{-1}), a high precision on its atomic coordinates cannot be expected. This is seen, for instance, with the rather short K−Ow distance [2.44(3) Å], which could not be improved by additional refinements. Nevertheless, the structure model is probably good enough for discussing the behavior of the water molecules during dehydration. Moreover, it is interesting to relate the number of water molecules (1.64) found from the structure Rietveld refinement to the water molecule amount derived from the hydration content dependence of the *c* parameter shown in Figure 11. Indeed, from the *c* parameter magnitude (8.4972 Å) for the partially dehydrated phase the expected hydration degree is 1.3 H_2O molecule. This value is in satisfactory agreement with the value derived from the structure refinement.

Description of the Structure. Figure 2b is a perspective view of the structure along the *c* axis. It shows that the framework of the structure is preserved during the dehydration process and the water molecules remain located in the tunnels. Nevertheless, the water content has a great influence on the distances observed both within the yttrium and potassium polyhedra and within the oxalate groups. As shown in Table 4, the release of some water molecules involves an elongation of Y−O1 and Y−O2 bond lengths and, consequently, increases the edge distances within the $[YO_8]$ dodecahedron. On the contrary, the K−O bond lengths decrease significantly. It might be due to the fact that the coordination environment of the potassium atoms contains on average less than six oxygen atoms. Similar

Table 4. Selected Bond Distances (Å) and Angles (deg) for $YK(C_2O_4)_2.1.64H_2O$[a]

Y−O1, O1^{i}, O1^{ii}, O1^{iii}	2.37(1)	O1−O2^{ii}	3.04(2)
Y−O2, O2^{i}, O2^{ii}, O2^{iii}	2.446(7)	O2−O2^{i}	2.776(8)
K−O2^{ii}, O2^{iii}, O2^{iv}, O2^{v}	2.63(1)	O2^{iv}−Ow^{ix}	3.27(3)
K−Ow^{vi}, Ow^{vii}, Ow^{viii}, Ow^{ix}	2.44(3)	O2^{iv}−Ow^{vi}	3.32(2)
C−O1	1.26(1)	O2^{iv}−Ow^{viii}	2.61(3)
C−O2^{x}	1.234(9)	Ow^{vi}−O1	2.94(2)
C−C^{x}	1.47(1)	Ow−Ow^{vi}	2.09(4)
O1−O1^{ii}, O1^{iii}	3.42(2)	Ow−Ow^{ix}, Ow^{xi}	3.69(4)
O1−O2	2.69(1)	Ow−O1	2.92(2)
O1−O2^{iii}	3.14(2)		
O1−Y−O1^{ii}	92.6(9)	O1−C−O2^{x}	118(1)
O1−Y−O2	67.8(4)	O2^{ii}−K−O2^{iii}	63.7(3)
O1−Y−O2^{iii}	81.3(7)	O2^{ii}−K−Ow^{vii}	62(1)
O1−Y−O2^{ii}	78.4(7)	O2^{ii}−K−Ow^{ix}	142(1)
O2−Y−O2^{i}	69.1(3)	O2^{ii}−K−Ow^{vi}	80(1)
O1−C−C^{x}	111(1)	Ow^{vi}−K−Ow^{viii}	98(1)
O2^{x}−C−C^{x}	125(1)		

[a] (i) $-x, {}^1/_2 - y, z$; (ii) $-{}^1/_4 + y, {}^1/_4 - x, {}^5/_4 - z$; (iii) ${}^1/_4 - y, {}^1/_4 + x, {}^5/_4 - z$; (iv) $x, y, -1 + z$; (v) $-x, {}^1/_2 - y, -1 + z$; (vi) ${}^1/_2 - x, {}^1/_2 - y, {}^1/_2 - z$; (vii) $-{}^1/_2 + x, y, {}^1/_2 - z$; (viii) ${}^1/_4 - y, -{}^1/_4 + x, -{}^1/_4 + z$; (ix) $-{}^1/_4 + y, {}^3/_4 - x, -{}^1/_4 + z$; (x) ${}^1/_2 - x, {}^1/_2 - y, {}^3/_2 - z$; (xi) ${}^3/_4 - y, {}^1/_4 + x, {}^1/_4 + z$.

features are observed within the oxalate groups. The water molecules are no longer hydrogen-bonded to the oxygen atoms from the adjacent water molecules in the tunnels, i.e., the distance between two water molecules increases from 2.937(8) Å in the tetrahydrate oxalate to 3.69(4) Å in $YK(C_2O_4)_2 \cdot 1.64H_2O$.

5. Concluding Remarks

The present study allows the detailed interpretation of the crystal structures and dehydration process of the mixed oxalates $YK(C_2O_4)_2.nH_2O$ ($4 > n > 0.5$). The power of modern powder diffraction is highlighted by the crystal structure of $YK(C_2O_4)_2 \cdot 4H_2O$ determined ab initio and the structure of $YK(C_2O_4)_2 \cdot 1.64H_2O$ refined from powder diffraction data collected with a monochromatic radiation obtained from a conventional X-ray source. The precision reached in the structure determination of the tetrahydrated phase is worth noting, since the H atoms have been located, which is not evident in the presence of heavy atoms, such as Y and K. The consequence on the precision of the bond lengths in the oxalate group has been clearly demonstrated. However, it should be noted that long ago the localization of Li atoms in the structures of two high-pressure phases of Li_2WO_4 solved from powder diffraction data were reported.[31] The use of temperature-dependent powder diffraction, combined with the data obtained from conventional thermal analysis has clearly pointed out the deformation of the open-framework oxalate structure during the reversible dehydration−hydration process. The crystal structure explains the origin of the zeolitic properties of the water molecules located in the channels. Furthermore, the precise measurements obtained from the thermal analyses have allowed the calculation of thermodynamic values for the dehydration process. It should also be noted that the water molecule content of the partially hydrated phases is correlated to the unit cell parameters.

In the recent years, the thermal behavior of the mixed oxalates of the series $K_3Ln(C_2O_4)_3.nH_2O$ and $K_8Ln_2(C_2O_4)_7 \cdot 14H_2O$ has been reported.[32] The presence of some zeolitic water molecules in the structures was supposed, but no further investigations could confirmed this observation. On the contrary, the present study has clearly demonstrated the existence of zeolitic water molecules in $YK(C_2O_4)_2 \cdot 4H_2O$. To our knowledge, it is the first example with this property among mixed oxalates derived from yttrium or rare earths and monovalent cations. A review of the crystal structure of these compounds shows that the unusual coordination number eight for yttrium or lanthanide is encountered only in the crystal structures of $K_8Ln_2(C_2O_4)_7 \cdot 14H_2O$ and $YK(C_2O_4)_2 \cdot 4H_2O$. The other mixed oxalate salts are characterized by 9-fold coordinated lanthanide or yttrium atoms, the coordination polyhedron being either a monocapped antiprism for most of them or a tricapped trigonal prism. The coordination environment of the yttrium or the lanthanide atoms in $K_8Ln_2(C_2O_4)_7 \cdot 14H_2O$ and $YK(C_2O_4)_2 \cdot 4H_2O$ has the form of a slightly distorted dodecahedron, built from oxalate oxygen atoms only. It seems that the absence of water molecules in the environment of the trivalent cation gives this geometry, instead of the Archimedean antiprism or the bicapped trigonal prism which can be obtained by removing one oxygen atom from the polyhedra available from 9-fold coordinated atoms.

Acknowledgment. The authors are indebted to G. Marsolier for his technical assistance in diffraction data collection.

CM981155X

(31) Waltersson, K.; Werner, P.-E.; Wilhelmi, K.-A. *Cryst. Struct. Commun.* **1977**, *6*, 225−230; *Cryst. Struct. Commun.* **1977**, *6*, 231−235.

(32) Kahwa, I. A.; Selbin, J. *J. Therm. Anal.* **1983**, *28*, 359−370.